Journal of Power Sources 245 (2014) 927–936

Contents lists available at SciVerse ScienceDirect

Journal of Power Sources

journal homepage: www.elsevier.com/locate/jpowsour

Clean hydrogen generation through the electrocatalytic oxidation of ethanol in a Proton Exchange Membrane Electrolysis Cell (PEMEC): Effect of the nature and structure of the catalytic anode

Claude Lamy [a,c], Thomas Jaubert [b], Stève Baranton [b,c], Christophe Coutanceau [b,c,*]

[a] Institut Européen des Membranes, UMR CNRS n°5635, Université de Montpellier 2, 2 Place Eugène Bataillon, 34095 Montpellier Cedex, France
[b] Université de Poitiers, Laboratory of Catalysis and Non-Conventional Media, IC2MP, CNRS UMR 7285, 4 rue Michel Brunet, 86022 Poitiers Cedex, France
[c] Groupe de Recherches PACS, CNRS GDR 3339, Université de Montpellier 2, France

HIGHLIGHTS

- Thermodynamics make ethanol a convenient biomass source for producing pure hydrogen.
- Pt-based catalysts are active and stable for the anodic oxidation of ethanol.
- Modification of Pt by Sn and Ru/Sn increases the faradic efficiency.
- High reaction rates at relatively low overvoltages have been achieved in a PEMEC.
- 50% electrical energy saving with ethanol decomposition vs. water electrolysis.

ARTICLE INFO

Article history:
Received 28 October 2012
Received in revised form
14 June 2013
Accepted 2 July 2013
Available online 17 July 2013

Keywords:
Electrolysis
Ethanol
Hydrogen generation
Pt-based catalysts

ABSTRACT

The electrocatalytic oxidation of ethanol was investigated in a Proton Exchange Membrane Electrolysis Cell (PEMEC) working at low temperature (20°C) on several Pt-based catalysts (Pt/C, PtSn/C, PtSnRu/C) in order to produce very clean hydrogen by electrolysis of a biomass compound. The electrocatalytic activity was determined by cyclic voltammetry and the rate of hydrogen evolution was measured for each catalyst at different current densities. The cell voltages U_{EtOH} were recorded as a function of time for each current density. At 100 mA cm^{-2}, i.e. 0.5 A with the 5 cm^2 surface area PEMEC used, the cell voltage did not exceed 0.9 V for an evolution rate of about 220 cm^3 of hydrogen per hour and the electrical energy consumed was less than 2.3 kWh $(Nm^3)^{-1}$, i.e. less than one half of the energy needed for water electrolysis (4.7 kWh $(Nm^3)^{-1}$ at $U_{H2O} = 2$ V). This result is valid for the decomposition of any organic compound, particularly those originated from biomass resource, provided that their electro-oxidation rate is sufficient (>100 mA cm^{-2}) at a relatively low cell voltage ($U_{cell} < 1$ V) which necessitates the development of efficient electrocatalysts for the electrochemical decomposition of this compound.

1. Introduction

The development of clean power sources and the reduction of the emission of greenhouse gases (e.g. carbon dioxide) have led to many investigations on Fuel Cells fed either with pure hydrogen [1] or with other fuels, particularly liquid fuels such as methanol [2] or ethanol [3].

The electrocatalytic oxidation of alcohols in a Direct Oxidation Fuel Cell (DOFC) such as a Direct Methanol Fuel Cell (DMFC) or a Direct Ethanol Fuel Cell (DEFC) is still limited due to the rather poor reactivity of these alcohols at relatively low temperatures (20–120 °C). The use of ethanol in a fuel cell (DEFC) system is particularly challenging since ethanol is a liquid fuel (with a rather high energy density of 8 kWh kg^{-1}), which can be produced from biomass feedstock (dedicated crops, grain, corn, root beet, etc.) or from different wastes by enzymatic hydrolysis and fermentation. However the electrical performances of a DEFC ($P_{max} \approx 0.1$ W cm^{-2}) are still lower by one order of magnitude than those of a PEMFC fed with pure hydrogen ($P_{max} \approx 1$ W cm^{-2}). Therefore, in order to use primary energy sources from biomass, such as ethanol, one way is to transform them into hydrogen by their electrochemical decomposition with electricity coming from nuclear power plants, or from renewable energy sources, such as hydroelectric power, wind turbines, solar photovoltaic, etc.

* Corresponding author. Université de Poitiers, Laboratory of Catalysis and Non-Conventional Media, IC2MP, CNRS UMR 7285, 4 rue Michel Brunet, 86022 Poitiers Cedex, France.
E-mail address: Christophe.Coutanceau@univ-poitiers.fr (C. Coutanceau).

0378-7753/$ – see front matter © 2013 Elsevier B.V. All rights reserved.
http://dx.doi.org/10.1016/j.jpowsour.2013.07.028

The production of hydrogen by water electrolysis is the most developed process, leading to high purity hydrogen, suitable to feed a low temperature Fuel Cell, such as a PEMFC or an AFC [1,4–7], leading to commercial electrolysers [8] with a relatively good energy efficiency (60–70%). Most of the anode catalysts are based on valve oxides (IrO_2, RuO_2, TaO_2) supported on a titanium sheet, similar to DSA type electrodes developed for the chloro-alkali industry. But the overvoltage of the Oxygen Evolution Reaction (OER) was never decreased below 0.5 V (i.e. a cell voltage of at least 1.7–1.8 V at 1 A cm^{-2}) [9].

Thus due to the high overvoltages encountered in water electrolysis, particularly at the catalytic anode, where oxygen evolution does occur, the production cost is actually not competitive with the main production processes (methane steam reforming, partial oxidation, auto thermal reforming) from natural gas [10]. This is because the energy needed to produce 1 kg of hydrogen is much greater than the theoretical energy (33 kWh kg^{-1} under standard conditions), reaching more than 50 kWh kg^{-1} (corresponding to about 4.5 kWh Nm^{-3}), i.e. an energy efficiency lower than 66%.

Therefore another approach, using biomass feedstock (instead of water) as a hydrogen source, seems to be very promising, since the theoretical cell voltage for the electrochemical decomposition of such compounds with hydrogen production is lower than the theoretical cell voltage of water electrolysis (1.23 V under standard conditions). Several organic feedstocks from biomass resource, like alcohols, carboxylic acids, sugars, etc., have been considered as sources of hydrogen, but relatively few works could be found in the literature on the electrochemical decomposition of organic compounds [11]. In particular, methanol [12–14], ethanol [15–17], glycerol [18,19], glucose [18] and formic acid [20,21] have been considered for hydrogen production through their electrolysis.

If most of the electrochemical decomposition reactions of these compounds have a low cell voltage (under standard conditions) they lead usually to larger cell voltages, under working conditions, due to high anodic overvoltages. This is particularly true for the electro-oxidation of low weight alcohols at bulk or nanodispersed pure platinum catalysts, which experience strong surface poisoning by CO coming from the dissociative chemisorption of the alcohol.

In this paper the feasibility of the production with higher rate of clean hydrogen by the electrolysis of ethanol in a Proton Exchange Membrane Electrolysis Cell (PEMEC) has been demonstrated. Different Pt-based catalysts have been investigated for the anodic oxidation of ethanol leading to high reaction rates at relatively low overvoltages, of the order of 0.8–0.9 V at 100 mA cm^{-2}, as experienced in a Direct Ethanol Fuel Cell [22].

2. Principle of ethanol decomposition in a PEMEC

The principle of the electrochemical decomposition of ethanol in a PEMEC is similar to that of water (Fig. 1).

In water electrolysis liquid or gaseous water is fed to the anodic compartment where it is oxidized producing oxygen and protons, i.e.:

$$H_2O \rightarrow \tfrac{1}{2}O_2 + 2H^+ + 2e^- \quad (1)$$

Oxygen evolves in the gaseous phase, whereas the electrons circulate in the external circuit and protons cross-over the membrane, reaching the cathodic compartment where they are reduced by the electrons coming from the external circuit, thus producing hydrogen, as follows:

$$2H^+ + 2e^- \rightarrow H_2 \quad (2)$$

This corresponds to the overall decomposition of water into hydrogen and oxygen:

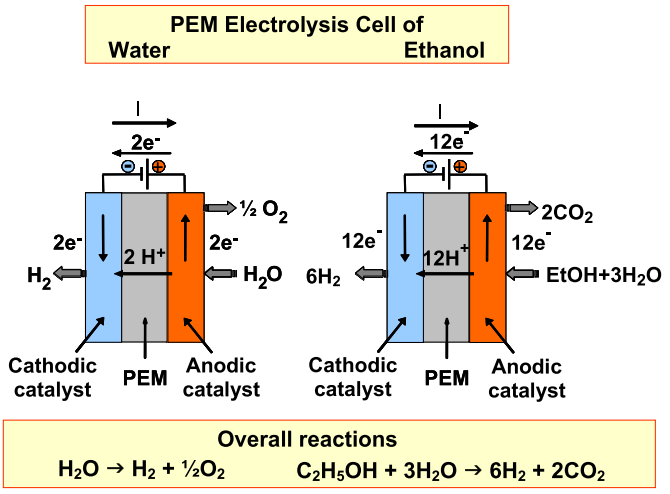

Fig. 1. Schematic principle of the electrochemical decomposition of water and ethanol in a Proton Exchange Membrane Electrolysis Cell (PEMEC).

$$H_2O \rightarrow H_2 + \tfrac{1}{2}O_2 \quad (3)$$

with $\Delta H = +285.8$ kJ (mole H_2O)$^{-1}$ and $\Delta G = +237.1$ kJ (mole H_2O)$^{-1}$ under standard conditions.

Similarly ethanol is fed to the anodic compartment where it can be completely oxidized in the presence of water, producing carbon dioxide and protons, i.e.:

$$C_2H_5OH + 3H_2O \rightarrow 2CO_2 + 12H^+ + 12e^- \quad (4)$$

and the protons, which reach the cathode compartment after crossing-over the membrane, are reduced to hydrogen according to reaction (2).

This corresponds to the electrochemical reforming of ethanol into hydrogen and carbon dioxide, according to the overall reaction:

$$C_2H_5OH + 3H_2O \rightarrow 6H_2 + 2CO_2 \quad (5)$$

with the thermodynamic data under standard conditions:

$\Delta H = +348$ kJ (mole ethanol)$^{-1}$ and $\Delta G = +96.9$ kJ (mole ethanol)$^{-1}$.

Both reactions need external energy ($\Delta H > 0$), coming from the external electrical power sources, but in the case of ethanol the energy needed to produce one hydrogen mole is much smaller: $\Delta H = +58$ kJ (mole H_2)$^{-1}$ for ethanol vs. $\Delta H = +286$ kJ (mole H_2)$^{-1}$ for water.

The corresponding theoretical cell voltage U_{cell}, under standard conditions, can be calculated from ΔG, i.e. $U_{cell} = \Delta G/nF^{-1}$, giving respectively:

$U_{H2O} = 1.229$ V for water electrolysis ($n = 2$) and $U_{EtOH} = 0.084$ V for ethanol decomposition ($n = 12$). For the Direct Ethanol Fuel Cell (DEFC), this corresponds to a standard cell voltage $E_{DEFC} = U_{H2O} - U_{EtOH} = 1.229 - 0.084 = 1.145$ V.

However the relatively slow kinetics of the anodic reaction in both processes, where high current densities (over 1 A cm^{-2}) are necessary for high hydrogen production rates, lead to high anodic potentials, greater than 1.8 V/SHE, in the case of water electrolysis, and at least 0.6 V/SHE for ethanol oxidation [22], where SHE stands for the Standard Hydrogen Electrode used as a reference electrode. This is illustrated in Fig. 2, where the $j(E)$ curves representative of the Butler–Volmer kinetics law are presented for the water

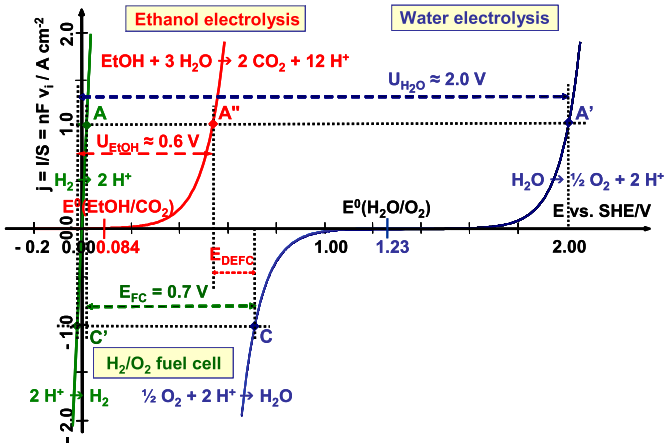

Fig. 2. Comparison of the theoretical j (E) electric characteristics representative of the Butter–Volmer kinetics law for water oxidation, ethanol oxidation, oxygen reduction and proton reduction. (U_{H2O}), (U_{EtOH}) and (E_{FC}) are the cell voltages for water electrolysis, ethanol electrolysis and hydrogen/oxygen fuel cell at a current density of 1 A cm^{-2}, respectively. $E^0(H_2O/O_2) = 1.23$ V/SHE and $E^0(EtOH/CO_2) = 0.084$ V/SHE are the standard electrode potentials of the electrochemical reactions involved.

oxidation reaction, the ethanol oxidation reaction, the hydrogen oxidation reaction (positive current densities), the oxygen reduction reaction and the proton reduction reaction (negative current densities); from these curves, the cell voltages for water electrolysis (U_{H2O}), ethanol electrolysis (U_{EtOH}), hydrogen/oxygen fuel cell (E_{FC}) and Direct Ethanol Fuel Cell (E_{DEFC}) at a current density of 1 A cm^{-2}, can be evaluated.

In order to get a competitive cost of energy for the production of hydrogen, the cell voltages have to be decreased down to acceptable values, through the development of new electrocatalysts with higher activity and selectivity. Indeed, the energy consumed is directly proportional to the cell voltage, according to Eq. (6):

$$W_e\left(\text{in kWh/Nm}^3\right) = \frac{\tilde{n}F}{3600V_m \times 10^3} U_{cell}(j) \approx 2.364\ U_{cell}(j) \quad (6)$$

where $V_m = 22.675 \times 10^{-3}$ m^3 mol^{-1} is the molar volume of an ideal gas at a temperature of 0 °C and under a pressure of 10^5 Pa (standard conditions for gaseous species) [23], $F = 96485$ C per mole of electron is the Faraday constant and $\tilde{n}$ is the average number of Faradays per mole of hydrogen involved in the overall process ($\tilde{n} = 2$ in both cases). For an ideal gas under normal conditions ($T = 273.15$ K, $P = 1$ atm $= 101.325$ kPa) the molar volume is $V_m = 22.414 \times 10^{-3}$ m^3 mol^{-1}, so that $W_e = 2.39$ kWh (Nm^3)$^{-1}$ per Volt. Since the electrical energy consumed depends only on the cell voltage $U_{cell}(j)$, where j is the current density, U_{cell} must be below 1 V to decrease the energy consumed below 2.4 kWh (Nm^3)$^{-1}$.

3. Experimental

3.1. Preparation of the catalysts

The mono- and multi-metallic catalyst colloidal precursors were synthesized using a procedure derived from the Bönnemann method [24,25]. This method was already developed in our Laboratory since a long time, so that we gained a long experience in using it for the preparation of multi-metallic electrocatalysts. Hence, we can compare results obtained in the present work with those obtained previously for the Direct Ethanol Fuel Cell working under similar conditions [22].

The synthesis is carried out under controlled atmosphere (argon) free of oxygen and water, with non-hydrated metal salts (99.9% $PtCl_2$, $RuCl_3$ and $SnCl_2$ from Alfa Aesar). The tetraalkyl triethylborohydride reducing agent, $(Nalk_4)^+(BEt_3H)^-$, was first synthesized. This reactant will also act as a surfactant after metal reduction, preventing any particle agglomeration after the formation of colloidal particles, according to the following reaction:

$$MeCl_n + n\ (Nalk_4)^+(BEt_3H)^- \rightarrow Me[(Nalk_4)^+Cl^-]_n + n\ BEt_3 + (n/2)\ H_2$$

The colloidal precursors are then dispersed on a carbon support (Vulcan XC 72) and calcined at 300 °C for 1 h under air atmosphere to remove the organic surfactant.

The synthesis of $Pt_{90}Sn_{10}$/C and $Pt_{86}Sn_{10}Ru_4$/C catalysts was carried out by coreduction of the different metal salts during the formation of the colloidal precursor according to the following equation:

$$x\ PtCl_2 + y\ MCl_n + (2x + ny)\ [(Nalk_4)^+(BEt_3H)^-] \rightarrow Pt_xM_y\ [(Nalk_4)^+Cl^-]_{(2x+ny)} + (2x + ny)\ BEt_3 + ((2x + ny)/2)\ H_2 \quad (7)$$

3.2. Characterization of the Pt-based catalysts

The synthesized catalysts were characterized by differential thermal analysis and thermogravimetric analysis (DTA-TGA), TEM, XRD, inductively coupled plasma optical emission spectroscopy (ICP-OES), and electrochemical methods.

Transmission electron microscopy (TEM) characterization was performed using a JEOL JEM 2010 (HR) microscope (0.35 nm resolution) with an EDX analyser equipped with a LaB_6 filament. The mean particle size and size distribution were determined by measuring the diameter of ca. 500 isolated particles using ImageJ free software [26].

Powder X-ray diffraction (XRD) patterns were recorded on a Bruker D5005 Bragg–Brentano (θ–θ) diffractometer operated with a copper tube powered at 40 kV and 40 mA ($CuK_{\alpha 1} = 1.54060$ Å and $CuK_{\alpha 2} = 1.54443$ Å). Measurements were carried out from $2\theta = 15°$ to $2\theta = 90°$ in a step mode, with steps of 0.06° and a fixed acquisition time of 10 s/step.

For electrochemical characterization, catalytic powders were deposited on a glassy carbon substrate according to a method used by Gloaguen et al. [27]. The catalytic powder (25 mg) is added to a mixture of 0.5 mL of a Nafion solution (5 wt.% from Aldrich) in ultrapure water. After ultrasonic homogenization of the catalyst/XC72-Nafion ink, a given volume is deposited from a syringe onto a freshly polished glassy carbon substrate yielding a catalytic powder loading of 354 μg cm^{-2}. The solvent is then evaporated in a stream of ultrapure nitrogen at room temperature. By this way, a catalytic layer is obtained with a thickness of ca. 1–1.5 μm. The electrochemical set-up consists in a Voltalab PGZ 402 computer-controlled potentiostat. The solutions were prepared from 0.1 M $HClO_4$ (suprapur, Merck), 0.1 M ethanol (97%, Alfa Aesar) and ultrapure water (18.2 MΩ cm). The electrochemical experiments were carried out at 20 °C in a N_2-purged supporting electrolyte, using a conventional thermostated three-electrode electrochemical cell. The working electrode was a glassy carbon disk (0.071 cm^2 geometric surface area), the counter electrode was a glassy carbon plate (8 cm^2 geometric surface area), and the reference electrode was a reversible hydrogen electrode (RHE).

3.3. MEA fabrication and electrolysis tests

The electrolysis cell tests in a single PEMEC with a 5 cm^2 geometric surface area were carried out by one-pass feed of the anode with a 2 M ethanol aqueous solution and the cathode with an acidic

solution (0.5 M H_2SO_4) at a flow rate of 2 mL min^{-1}. The $U_{cell}(t)$ and $U_{cell}(j)$ curves were recorded using a DC Power Supply (E3614A from Agilent) to fix the current and Digital Multimeters (34405 A from Agilent) to record the cell voltage and the applied current density. The volume of generated H_2 was measured by a gas volumeter consisting in the water displacement in a graduated glass tube connected to the cell. The experimental set-up is schematized in Fig. 3.

Carbon gas diffusion electrodes were homemade using a carbon cloth from Electrochem Inc. on which was brushed an ink made of Vulcan XC 72 carbon powder and PTFE dissolved in isopropanol. The gas diffusion electrodes were loaded with 4 mg cm^{-2} of a mixture of carbon powder and 20 wt.% PTFE. Electrodes for PEMEC were prepared from an ink consisting in a mixture of Nafion (5 wt.% from Aldrich) solution, water and catalytic powder, dried on a carbon gas diffusion electrode. The metal loading of the electrodes was close to 2.0 mg cm^{-2} and the Nafion loading of the electrode was ca. 0.8 mg cm^{-2}. The MEAs were prepared, by hot pressing at 130 °C for 90 s under a pressure of 35 kg cm^{-2} a pre-treated Nafion 117 membrane with a cathode (2.0 mg cm^{-2} Pt loading, 30 wt.% Pt on carbon, 20 wt.% PTFE, 0.8 mg cm^{-2} Nafion) and an anode (2.0 mg cm^{-2} metal loading, 30 wt.% metal on carbon, 20 wt.% PTFE, 0.8 mg cm^{-2} Nafion).

4. Results and discussion

4.1. Physicochemical characterization and electrocatalytic activity of Pt-based alloys towards the oxidation of ethanol

The catalyst compositions used in the present work were chosen according to previous studies made in our laboratory on ethanol electro-oxidation. It was clearly shown that, using the Bönnemann method for the synthesis of catalysts, $Pt_{0.9}Sn_{0.1}$ and $Pt_{0.86}Sn_{0.1}Ru_{0.04}$ with such atomic ratios, led to higher activity towards the electrooxidation of ethanol [22,28].

The main information obtained from the characterization of monometallic Pt/C, bimetallic $Pt_{90}Sn_{10}$/C and trimetallic $Pt_{86}Sn_{10}Ru_4$/C catalysts are that the synthesis method led to metal loadings as determined by TDA-TGA measurements very close to the nominal one (30 wt.%), and that the catalyst compositions as determined by ICP-OES and EDX measurements are also in agreement with the nominal ones. Although EDX measurement in three different zones of the catalyst gave ratios close to the nominal one, only a very small shift in the diffraction peaks of the XRD pattern was observed (Table 1). The synthesis method does not allow alloying completely tin with platinum, as it can be seen by comparing the cell parameter of a synthesized Pt_3Sn/C catalyst with a commercial one. This clearly shows that some alloying is obtained during the coreduction process of Pt and Sn. The average crystallite size calculated from the Scherrer formula using the width of the best-resolved diffraction peak at half height gives a value of 2.6 nm in good agreement with TEM analyses which show that the particle size is well distributed around a mean value of 2.6 ± 1.3 nm (Fig. 4).

Table 1
2θ values at the maximum of the (220) diffraction peak and cell parameters for different $Pt_{1-x}Sn_x$/C catalysts.

Catalysts	(220) diffraction peak position/2θ°	Cell parameter/Å
Pt/XC72 30%	67.3	3.932
$Pt_{90}Sn_{10}$/C 30%	67.168	3.939
$Pt_{75}Sn_{25}$/C 30%	67.223	3.936
$Pt_{75}Sn_{25}$/C 20%	66.666	3.965
Pt_3Sn/C 20% E-Tek	66.029	3.999

The electrocatalytic oxidation of ethanol has been investigated for many years on several platinum-based electrodes, including Pt/X alloys (with X = Ru, Sn, Mo, etc.), and dispersed nanocatalysts. Pure platinum smooth electrodes are rapidly poisoned by some strongly adsorbed intermediates, such as carbon monoxide, resulting from the dissociative chemisorption of the molecule, as shown by the first experiments in infrared reflectance spectroscopy [29]. Both kinds of adsorbed CO, either linearly-bonded or bridge-bonded to the platinum surface, are observed. Besides, other adsorbed species have been identified by IR reflectance spectroscopy, and liquid chromatography [30], including reaction intermediates, such as acetaldehyde and acetic acid, and other by-products.

It has already been well established that the modification of Pt by Sn led to a great improvement in the catalytic activity towards the ethanol electroxidation reaction, in particular for Sn/Pt ratio lower than 0.3 [28,31]. Kim et al. prepared alloyed PtSn catalysts with different Pt/Sn ratios. They found the highest catalytic activity for a Pt/Sn atomic ratio of ca. 1:1, but with catalysts of different structure than those used in our studies, and concluded that a compromise between composition and structure is a key factor for catalytic activity improvement [32]. Rousseau et al. also showed that addition of ruthenium to a PtSn anode catalyst allowed achieving a maximum power density in a Direct Ethanol Fuel Cell twice higher than that obtained with a PtSn anode catalyst alone, giving ca. 30 mW cm^{-2} with a $Pt_{90}Sn_{10}$/C anode to ca. 60 mW cm^{-2} with a $Pt_{86}Sn_{10}Ru_4$ anode [22]. The modification of PtSn or $PtSnO_2$ by Rh is also investigated [33] because previous studies showed that Rh facilitated the C–C bond cleavage leading to increase the CO_2 yield [34,35]. But, the addition of Rh to PtSn does not increase the current of ethanol electrooxidation [36,37], conversely to the addition of ruthenium.

Cyclic voltammograms were recorded in a 3-electrode cell containing a 0.1 M $HClO_4$ + 0.1 M C_2H_5OH solution with Pt/C, $Pt_{90}Sn_{10}$/C and $Pt_{86}Sn_{10}Ru_4$/C electrodes and confirmed previous results (Fig. 5) [28]. The oxidation of ethanol starts at ca. 0.4 V vs. RHE on pure Pt and ca. 0.2 V vs. RHE on both $Pt_{90}Sn_{10}$ and $Pt_{86}Sn_{10}Ru_4$ catalysts. But, the ternary catalyst leads to higher current density over the whole studied potential range, which shows its higher catalytic activity towards ethanol electro-oxidation. Investigations by Kim et al. on the electrocatalytic oxidation of ethylene glycol and glycerol on a carbon-supported PtRuSn/C catalyst showed that the modification of PtSn by Ru led to the efficient oxidative removal of poisoning CO species produced during the oxidation reaction. Consequently, significant enhancement of the electrocatalytic activity and stability could be achieved. Such behaviour could also be involved in the electrooxidation of ethanol [38].

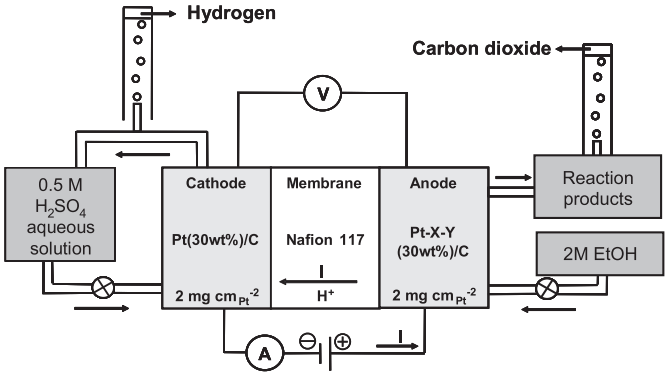

Fig. 3. Experimental set-up for the study of the ethanol electrolysis reaction in a PEMEC and for hydrogen evolution measurements; Pt-*X*-*Y* electrocatalysts with *X*, *Y* = Sn and/or Ru.

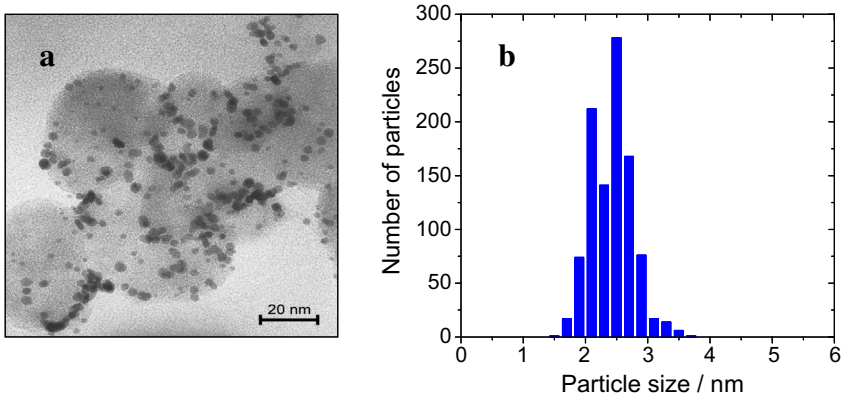

Fig. 4. (a) TEM image of a Vulcan supported $Pt_{90}Sn_{10}$/C catalyst (with a metal loading of 30%) prepared by the colloidal method; (b) particle size distribution (based on the observation of 500 particles).

Voltammetric results, completed by the different spectroscopic and chromatographic results, allowed us to propose a detailed reaction mechanism of ethanol oxidation, involving parallel and consecutive reactions, on Pt-based electrodes (such as PtSn catalysts), where the key role of the adsorption steps was underlined.

Since it is relatively difficult to oxidize completely ethanol into carbon dioxide at room temperature, two main parallel reaction paths, leading to the formation of intermediate products (acetaldehyde AL or acetic acid AA) have been considered:

$$CH_3CH_2OH \rightarrow CH_3CHO + 2H^+ + 2e^- \quad (\text{reaction rate } v_1) \qquad (8)$$

or

$$CH_3CH_2OH + H_2O \rightarrow CH_3COOH + 4H^+ + 4e^- \quad (\text{reaction rate } v_2) \qquad (9)$$

Depending on the kind of electrocatalyst used and the electrode potential at which the reaction does occur, the reaction rate v_1 or v_2 controls the rate determining step (rds) leading predominantly either to AL or AA.

Further oxidation to CO_2 needs the presence of extra oxygen atoms provided by the oxidation of adsorbed water, according to the bifunctional mechanism [39]. This process is favoured on Pt-based electrocatalysts (Pt-X with X = Sn, Ru, etc.) at potentials (0.4–0.6 V vs. RHE) lower than those needed with Pt alone (0.6–0.8 V vs. RHE).

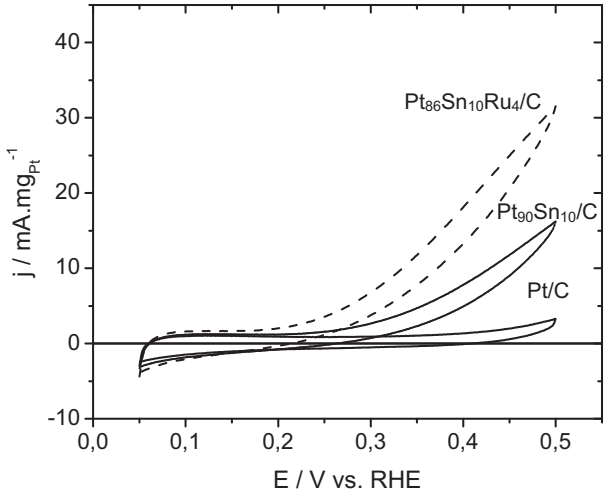

Fig. 5. Cyclic voltammograms recorded in a 0.1 M $HClO_4$ + 0.1 M ethanol solution on different Pt-based electrodes with a Pt loading of 0.1 mg_{Pt} cm^{-2} at v = 5 mV s^{-1} and T = 20 °C.

The reaction mechanism of ethanol oxidation on a Pt-based electrode can be summarized by the following scheme [40] (Scheme 1).

In this mechanism the adsorbed acetyl plays a key role and its further oxidation is favoured by the addition to platinum of metal atoms, such as Ru, Sn, Mo, etc., more easily oxidizable than Pt at low potentials.

This mechanism can explain the higher efficiency of PtSn in forming AA compared to Pt at low potentials (E < 0.5 V vs. RHE), as was shown by chronoamperometry and chronopotentiometry experiments [31]. Moreover adsorbed OH species on Sn atoms can oxidize-$(CH_3CO)_{ads}$ adsorbed acetyl species to CH_3COOH or CO species to CO_2, according to the bifunctional mechanism [39].

4.2. Electrolysis of ethanol in a Proton Exchange Membrane Electrolysis Cell (PEMEC)

4.2.1. Determination of the electrical characteristics of the electrolysis experiment

Electrolyses of 2 M ethanol were carried out in a PEMEC at 20 °C and two constant controlled current densities (j = 50 and 100 mA cm^{-2}) with three Pt-based electrocatalysts: Pt/C, $Pt_{90}Sn_{10}$/C and $Pt_{86}Sn_{10}Ru_4$/C. In each case the cell voltage U_{cell} was recorded as a function of time (t = 0–30 min) and the evolved hydrogen was measured with the gas flow meter. On the other hand the analysis of the reaction products was carried out by HPLC after 30 min of electrolysis at 100 mA cm^{-2}.

Fig. 6 shows the polarisation curves recorded for an electrolysis cell fitted with the different anode catalysts. The cell voltage U_{cell} vs. current density j curves display the expected logarithmic behaviour. The same behaviour is observed in the electrolysis cell as in the classical three-electrode electrochemical cell, e.g. both the binary and ternary catalysts lead to similar cell voltage at a given current density, lower than that achieved with the pure Pt catalyst in the low potential region. However in the high potential region, where the added elements (Sn, Ru) are no more stable and can dissolve, the $U_{cell}(j)$ curve of the $Pt_{90}Sn_{10}$/C catalyst is quite similar to that of the Pt/C catalyst.

The $U_{cell}(t)$ curves are given in Fig. 7 at 100 mA cm^{-2} for PtC and 50 and 100 mA cm^{-2} for the binary and ternary catalysts. It has to be stated that in the case of pure Pt, very important potential instabilities appeared for the experiment at 50 mA cm^{-2}, whereas in the case of the binary and ternary catalysts, short-period potential

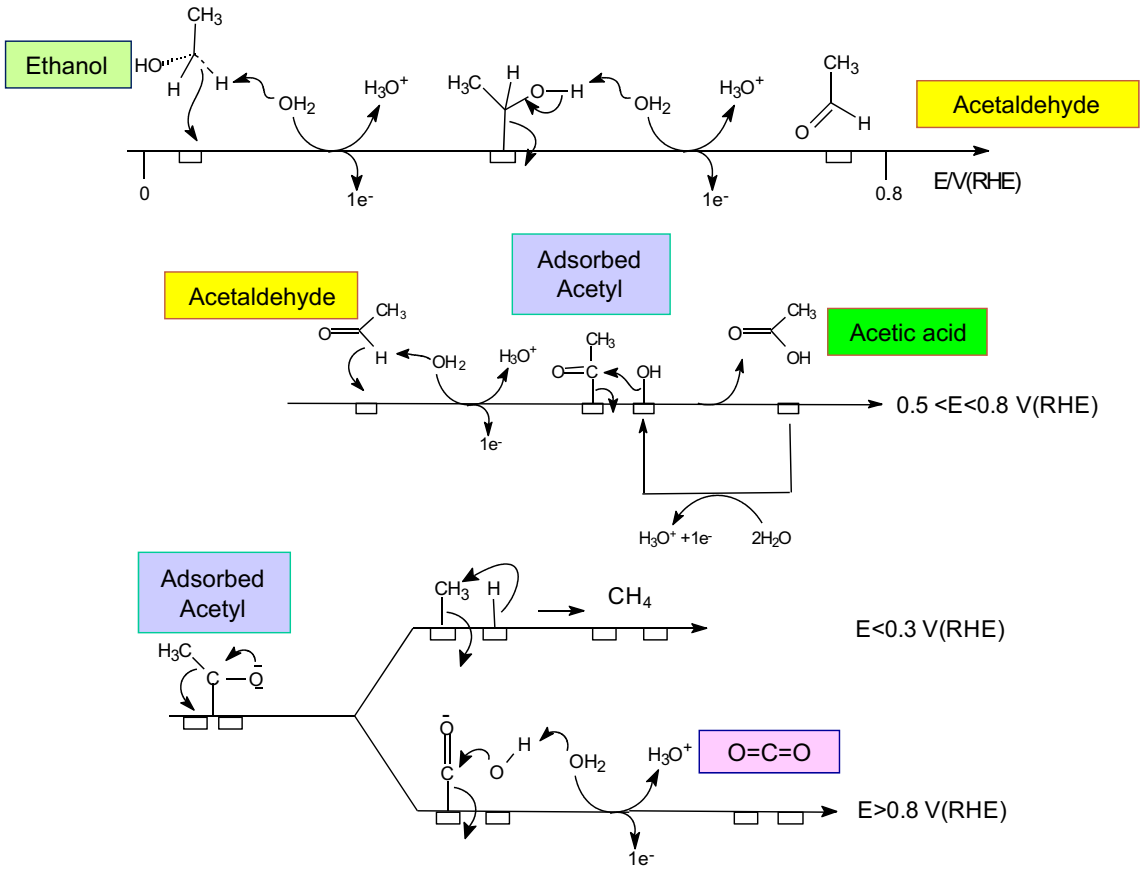

Scheme 1. Proposed mechanism for the electrocatalytic oxidation of ethanol on a Pt-based electrode in acidic medium (all the species with colour filling were detected either by *IR* reflectance spectroscopy anb/or by chromatographic analysis).

oscillations were observed (not shown here). For all catalysts, the cell voltage was always higher after 30 min of electrolysis than the initial values, independently of the current density used. This behaviour is not very interesting for long-term electrolysis, since U_{cell} increases continuously with time, leading to higher electrical energy consumption. This deactivation was due the formation of strongly adsorbed intermediates occurring during the electro-oxidation of ethanol, and it was possible to reactivate the catalysts by increasing the cell voltage up to 1.0 V. Under such anode potential conditions, previously adsorbed CO from the dissociative adsorption of ethanol is oxidized, and in the same time either no adsorbed CO is formed from ethanol adsorption, or the adsorbed CO oxidation kinetics is sufficiently fast to avoid its accumulation at the electrode surface and the blockage of the catalytic sites. Therefore, such treatment makes the catalyst surface clean. One can notice that this explanation is in agreement with the constant value of U_{cell} observed at ca. 1 V (for 100 mA cm^{-2}) on all catalysts, whereas some potential oscillations were observed for lower current density (50 mA cm^{-2}) between 0.6 and 0.75 V. Such oscillations were already observed for the oxidation of methanol, formic acid, formaldehyde, ethanol, propanol and other organic compounds at platinum-based electrodes in acidic as well as in alkaline media [41–47]. The occurrence of these oscillations was explained in terms of cycles of accumulation and consumption of adsorbed species (poisoning species, anions, oxygenated species) leading to instabilities in the steady state situation [48].

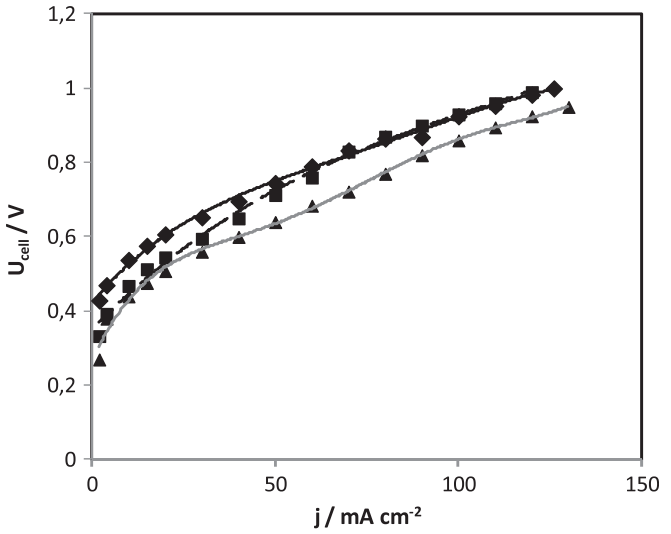

Fig. 6. Electrolysis cell voltage vs. current density, $U_{cell}(j)$, for the oxidation of 2 M CH_3CH_2OH in the PEMEC (0.5 M H_2SO_4, Pt/C, N117, $Pt_xSn_yRu_z$/C, 2 M CH_3CH_2OH, $V_{initial}$ = 1 L, flow rate = 2 mL min^{-1}) at 20 °C. ◆Pt/C anode, ■ $Pt_{90}Sn_{10}$/C anode, ▲ $Pt_{86}Sn_{10}Ru_4$/C.

4.2.2. Measurement of the hydrogen evolution rate

The hydrogen evolution rate was determined by measuring the volume of evolved hydrogen as a function of time for two different current densities (j = 50, and 100 mA cm^{-2}) during the electrolysis of a 2 M C_2H_5OH solution.

In all experiments the measured volume of hydrogen is a linear function of time (with correlation coefficients >0.9968) showing

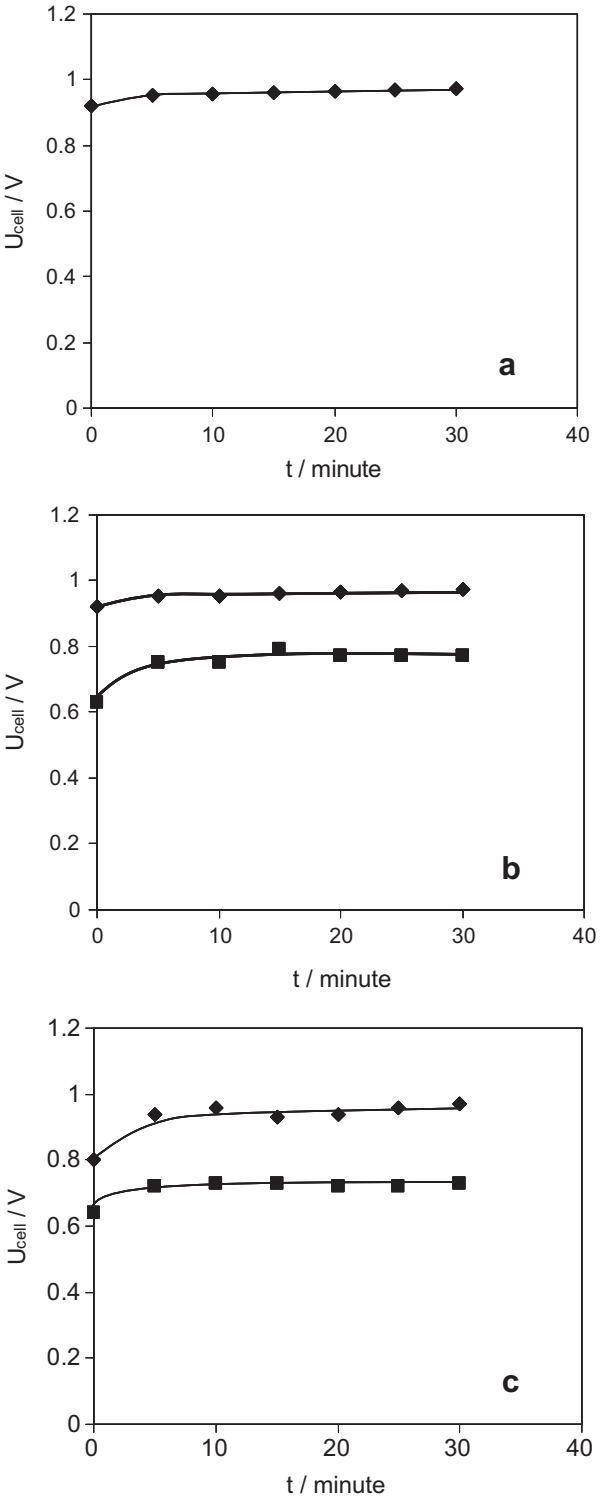

Fig. 7. Electrolysis cell voltage vs. time, $U_{cell}(t)$, at 20 °C for a PEMEC fitted with a Pt/C cathode and: (a) a Pt/C anode, (b) a $Pt_{90}Sn_{10}$/C anode and (c) a $Pt_{86}Sn_{10}Ru_4$/C anode. 2 M ethanol, $V_{initial}$ = 1 L, flow rate = 2 mL min^{-1}; ◆ j = 100 mA $cm^{-2}$and ■ j = 50 mA cm^{-2}.

clearly that the volume of evolved hydrogen does not depend on the C_2H_5OH concentration, nor on the nature of the anode catalyst, but only on the current intensity I (Fig. 8).

This proves that the process follows the Faraday's law according to the following equations:

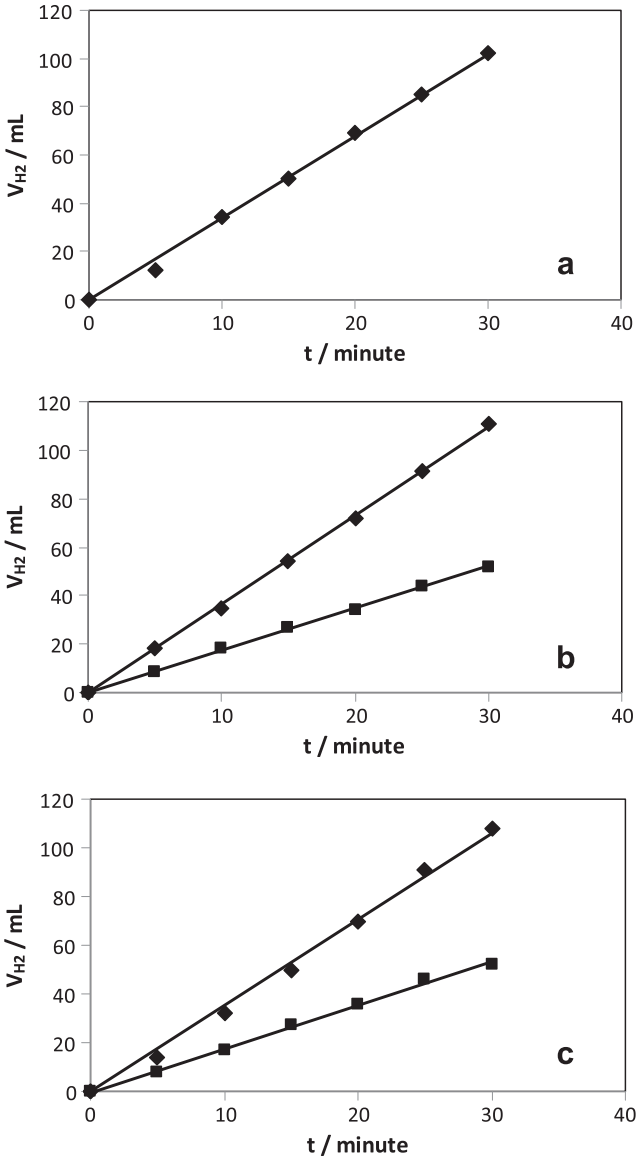

Fig. 8. Hydrogen evolution at different current density for the PEMEC (0.5 M H_2SO_4, Pt/C, N117, (a) Pt/C, (b) $Pt_{90}Sn_{10}$/C, (c) $Pt_{86}Sn_{10}Ru_4$/C), 2 M CH_3CH_2OH, $V_{initial}$ = 1 L, flow rate = 2 mL min^{-1} at 20 °C. ◆ j = 100 mA cm^{-2}, ■ j = 50 mA cm^{-2}.

$$dV_{H_2}/dt = V_{mol} dN_{H_2}/dt = V_{mol}(I/\tilde{n}F) \quad (10)$$

$$dV_{H_2}/dt = V_{mol}(I/2F) \times 60 = 7.61\, I\left(\text{in cm}^3\ \text{min}^{-1}\right) \quad (11)$$

where V_{mol} is the molar volume of hydrogen at a given temperature and pressure ($V_{mol} = 24.465 \times 10^{-3}$ m^3 $mole^{-1}$ at 20 °C and 1 bar), I is the current intensity expressed in Ampere and $\tilde{n} = 2$ is the number of Faraday per mole of hydrogen produced in the oxidation reaction of an ethanol molecule according to Eq. (4) (complete oxidation reaction to CO_2) or to Eqs. (8) or (9) (partial oxidation reactions to intermediate products).

Table 2 summarizes all the results obtained with the 3 electrocatalysts (Pt/C, $Pt_{90}Sn_{10}$/C and $Pt_{86}Sn_{10}Ru_4$/C) investigated here, where V_{H2} experimental is the volume of evolved hydrogen after 30 min electrolysis of 2 M ethanol at 100 mA cm^{-2}. These experimental results are compared to the calculated values of the volume of hydrogen produced after 30 min of electrolysis according to the

Table 2
Comparison of the experimental volume of hydrogen (V_{H2}) with the theoretical value.

Electrocatalyst	V_{H2} experimental/mL (after 30 min at 0.5 A)	V_{H2} theoretical/mL at 20 °C (after 30 min at 0.5 A)
Pt/C	102	112
PtSn/C	111	112
PtSnRu/C	108	112

Faraday's law (Eq. (10)). The agreement is very good in all experiments, but with experimental values slightly lower than those calculated, which may come from some gas leakage, either in the experimental set-up, or through the proton exchange membrane.

For all experiments the electrical energy needed to produce 1 Nm^3 of hydrogen was also evaluated, since it is only a function of the cell voltage U_{cell}, according to Eq. (6). The values obtained for U_{cell}, during ethanol electrolysis from 0 to 30 min, are given in Tables 3–5, together with the electrical energy used to produce 1 Nm^3 of hydrogen.

In all the results obtained the amount of electrical energy is below 2.3 kWh $(Nm^3)^{-1}$ (since $U_{cell} < 0.9$ V), which is at least 2 times lower than the energy consumed for water electrolysis.

4.2.3. Analysis of the reaction products of ethanol oxidation

In order to determine the reaction products, the current density was kept constant and the voltage of the cell was measured as a function of time. The ethanol flow rate was chosen at 2 mL min^{-1} in order to perform the experiments for 30 min. Because the electrodes are homemade, fluctuations in the amount of catalyst deposited on the electrode can occur. Then, in order to compare the behaviour of the different catalysts (Pt/C, $Pt_{90}Sn_{10}$/C and $Pt_{86}Sn_{10}Ru_4$/C) in terms of selectivity, it is preferable to express the selectivity as a non-dimensional parameter such as the ratio between the number of moles of a produced species to the total number of moles of all the formed products, which corresponds rather to the chemical yield for each reaction product.

Table 6 reports the results obtained at a current density of 100 mA cm^{-2} (i.e. a current intensity I = 0.5 A) for the three different catalysts. With all catalysts, only acetaldehyde (AL) and acetic acid (AA) were detected by chromatographic analyses. Thus the amount of CO_2 formed was estimated by comparing the faradic charge involved in the formation of AL and AA to the whole charge, Q, involved during the electrolysis experiment:

$$Q = I \times \Delta t = 0.5 \times 30 \times 60 = 900\ \text{C}.$$

From the results given in Table 6, it appears that the addition of tin to platinum greatly favours the cleavage of the C–C bond at such high anode potentials, the yield in CO_2 being more than twice higher with the $Pt_{90}Sn_{10}$/C and the $Pt_{86}Sn_{10}Ru_4$/C catalysts than with the Pt/C catalyst.

Furthermore the evaluation of the total number of Faradays per mole of ethanol exchanged during the oxidation process, i.e. $n_e = 3.5$ to 4.6 (Table 6), suggests that the main reaction product is acetic acid ($n_e \approx 4$). Thus, assuming that the mean number of Faraday per mole of ethanol is about 4 (as determined from the quantitative analysis of reaction products), i.e. that the oxidation of ethanol stops at acetic acid, the electrochemical reactions involved in the electrolysis process are:

$$CH_3CH_2OH + H_2O \rightarrow CH_3COOH + 4H^+ + 4e^- \quad (9)$$

and $4H^+ + 4e^- \rightarrow 2H_2$

corresponding to the overall reaction:

$$CH_3CH_2OH + H_2O \rightarrow CH_3COOH + 2H_2$$

with the following thermodynamic data under standard conditions :

$$\Delta H = +79.1\ \text{kJ mol}^{-1}; \Delta G = +22\ \text{kJ mol}^{-1}.$$

Then comparing the net energy obtained by the complete oxidation of ethanol to CO_2 ($\Delta H = -1366$ kJ mol^{-1}; $\Delta G = -1325$ kJ mol^{-1} [3,40]) to that obtained by its partial oxidation to acetic acid:

$$CH_3CH_2OH + O_2 \rightarrow CH_3COOH + H_2O$$

with $\Delta H = -492.5$ kJ mol^{-1}; $\Delta G = -452.2$ kJ mol^{-1},we still have a positive energy balance of 492.5 kJ mol^{-1} ethanol (in terms of combustion energy) and of 452.2 kJ mol^{-1} ethanol (in terms of electrical energy in a fuel cell). In other words, for the partial oxidation process, we have to supply 79.1 kJ mol^{-1} ethanol to decompose it into 1 mol of acetic acid and 2 mol of hydrogen, which

Table 3
Cell voltage, electrical energy, experimental and theoretical volume of generated H_2 as a function of time for the electrolysis of 2 M ethanol at 20 °C in a 5 cm^2 PEMEC under the same experimental conditions as in Fig. 7 for Pt/C (100 mA cm^{-2}).

Time/s	Cell voltage/V	Electrical energy/kWh $(Nm^3)^{-1}$	Volume of evolved H_2/mL	Theoretical volume of H_2 at 20 °C/mL
0	0.922	2.17	0	0
300	0.954	2.25	12	18.7
600	0.955	2.23	34	37.4
900	0.962	2.27	50	56.1
1200	0.965	2.28	69	74.8
1500	0.968	2.29	85	93.5
1800	0.972	2.30	102	112

Table 4
Cell voltage, electrical energy, experimental and theoretical volume of generated H_2 as a function of time for the electrolysis of 2 M ethanol at 20 °C in a 5 cm^2 PEMEC under the same conditions as in Fig. 7 for $Pt_{90}Sn_{10}$/C (100 mA cm^{-2}).

Time/s	Cell voltage/V	Electrical energy/kWh $(Nm^3)^{-1}$	Volume of evolved H_2/mL	Theoretical volume of H_2 at 20 °C/mL
0	0.920	2.17	0	0
300	0.951	2.25	18	18.7
600	0.958	2.26	35	37.4
900	0.960	2.27	54	56.1
1200	0.962	2.27	72	74.8
1500	0.968	2.29	91.5	93.5
1800	0.972	2.30	111	112

Table 5
Cell voltage, electrical energy, experimental and theoretical volume of generated H_2 as a function of time for the electrolysis of 2 M ethanol at 20 °C in a 5 cm^2 PEMEC under the same conditions as in Fig. 7 for $Pt_{86}Sn_{10}Ru_4$/C (100 mA cm^{-2}).

Time/s	Cell voltage/V	Electrical energy/kWh $(Nm^3)^{-1}$	Volume of evolved H_2/mL	Theoretical volume of H_2 at 20 °C/mL
0	0.80	1.90	0	0
300	0.94	2.22	14	18.7
600	0.96	2.27	32	37.4
900	0.93	2.20	50	56.1
1200	0.94	2.22	70	74.8
1500	0.96	2.27	91	93.5
1800	0.97	2.29	108	112

Table 6
Chemical yield, ethanol consumption and number of electrons exchanged per mole of ethanol for the electrolysis of 2 M ethanol at 0.5 A (j = 100 mA cm^{-2}).

Catalyst		AL	AA	CO_2	Ethanol consumed/mole	Calculated n_e[a]
Pt/C	$U_{cell} \approx$ 0.92–0.97 V					
	Amount of substance/mol	1.28×10^{-3}	1.16×10^{-3}	3.54×10^{-4}	2.62×10^{-3}	3.5
	Chemical yield/mol%	**46**	**42**	**12**		
$Pt_{0.9}Sn_{0.1}/C$	$U_{cel\ l} \approx$ 0.92–0.97 V					
	Amount of substance/mol	7.17×10^{-4}	9.63×10^{-4}	6.74×10^{-4}	2.02×10^{-3}	4.6
	Chemical yield/mol%	**30**	**41**	**29**		
$Pt_{0.86}Sn_{0.1}Ru_{0.04}/C$	$U_{cel\ l} \approx$ 0.80–0.96 V					
	Amount of substance/mol	9.52×10^{-4}	7.76×10^{-4}	7.20×10^{-4}	2.09×10^{-3}	4.5
	Chemical yield/mol%	**39**	**32**	**29**		

[a] Total number of mole of electrons exchanged for the oxidation of 1 mol of ethanol, assuming that no other electrolysis products than AL, AA and CO_2 are formed.

will provide $2 \times 285.8 = 571.6$ kJ by their combustion into oxygen giving 2 mol of water, i.e. a positive energy balance of 571.6–79.1 = 492.5 kJ mol^{-1} of ethanol. Of course the complete oxidation of ethanol to CO_2, which leads to 6 mol of hydrogen in the electrolysis process (see Eq. (5)), i.e. 3 mol of water in the fuel cell process, will give a much higher positive energy balance of 1366 kJ mol^{-1} ethanol (in terms of combustion energy) and of 1325 kJ mol^{-1} ethanol (in terms of electrical energy in a fuel cell).

The number of moles of ethanol transformed after 30 min of electrolysis can then be evaluated, assuming $n_e \approx 4$, as follows:

$$\Delta N = Q/n_eF = 900/(4*96485) = 2.33 \times 10^{-3}\text{mole} \qquad (12)$$

which corresponds to a very small fraction of ethanol converted, $\Delta N/N \approx 2 \times 10^{-2}$, for an initial solution containing 0.12 mol (2 mol L^{-1} at 2 mL min^{-1} for 30 min) and to low reaction rates v ($v = 2.33 \times 10^{-3}/1800 = 1.3 \times 10^{-6}$ mol s^{-1} = 4.66 mmol h^{-1}).

5. Conclusions

Beside water many other hydrogen containing compounds, in particular organic compounds from biomass resources, can generate hydrogen through their dissociation.

The electrochemical decomposition of water or of an organic compound gives hydrogen with a much higher purity than that obtained by thermal processes such as SR, ATR and PrOx, and there is no need to further clean-up the evolved gas, because no other gaseous species (such as CO, CO_2, etc.) than hydrogen are produced at the cathodic side of the PEMEC thanks to the properties of the separating Proton Exchange Membrane. Water electrolysis is a nearly mature process, but it needs a relatively high amount of energy ($\sim$5 kWh (Nm^3)$^{-1}$).

In this work, we gave new results on the feasibility of the production of clean hydrogen by the electrolysis of an organic compound, such as ethanol, in a Proton Exchange Membrane Electrolysis Cell (PEMEC):

- the thermodynamic characteristics of ethanol decomposition (U_{EtOH} = 0.084 V) make this organic compound a convenient biomass source for producing ultrapure hydrogen in a PEMEC;
- Pt-based catalysts are active and stable for the anodic oxidation of ethanol;
- high reaction rates at relatively low overvoltages, e.g. 0.8–0.9 V at 100 mA cm^{-2}, have been achieved in a PEMEC with platinum-based catalysts, consuming less than 2.3 kWh (Nm^3)$^{-1}$, i.e. more than one half of the electrical energy can be saved with ethanol decomposition in a PEMEC when compared to water electrolysis;
- some potential oscillations were observed at low current densities, which probably results from the presence of poisoning species, such as CO, coming from the dissociative chemisorption of ethanol.

One key point demonstrated in this work is the importance of the nature and structure of the electrocatalyst needed to reduce the overvoltage, η_a, of ethanol oxidation in order to decrease the operational cell voltage, i.e. to decrease the quantity of electrical energy needed for producing hydrogen through its electrochemical decomposition. In this respect the modification of Pt by Sn and/or Ru allowed us to decrease η_a, and thus to increase the current density, j, i.e. the rate at which gaseous hydrogen is produced. A final conclusion is that any organic compound will lead to similar results, since the rate of hydrogen evolution only depends on $\tilde{n}$, the average number of Faradays per mole of hydrogen involved in the overall process ($\tilde{n} = 2$ for any organic compound). Thus the most interesting compound from biomass resources will be that one with a lower thermodynamic cell voltage for its electrochemical decomposition, with the right choice of the best efficient electrocatalyst leading to the lowest overvoltage under working conditions of the electrolysis process.

Acknowledgements

The authors greatly acknowledge the CNRS Research Grouping PACS (GDR 3339) and the Institute of Chemistry of the "Centre National de la Recherche Scientifique" (CNRS) for supporting this work.

References

[1] B. Sørensen, Hydrogen and Fuel Cell Emerging Technologies and Applications, Elsevier Academic Press, New York, 2005.
[2] A. Arico, V. Baglio, V. Antonucci, Direct methanol fuel cells: history, status and perspectives, in: H. Zhang, H. Liu (Eds.), Electrocatalysis of Direct Methanol Fuel Cells, Wiley-VCH, Weinheim, 2009, pp. 1–78 (Chapter 17).
[3] C. Lamy, C. Coutanceau, J.-M. Léger, The direct ethanol fuel cell: a challenge to convert bioethanol cleanly into electric energy, in: P. Barbaro, C. Bianchini (Eds.), Catalysis for Sustainable Energy Production, Wiley-VCH, Weinheim, 2009, pp. 3–46 (Chapter 1).
[4] S. Grigoriev, V. Porembsky, V. Fateev, Int. J. Hydrogen Energy 31 (2006) 171.
[5] Y. Nishimura, K. Yasuda, Z. Siroma, K. Asaka, Denki Kagaku Oyobi Kogyo Butsuri Kagaku 65 (1997) 1122.
[6] P. Millet, F. Andolfatto, R. Durand, Int. J. Hydrogen Energy 21 (1996) 87.
[7] A. Marshall, Characterisation of Electrocatalysis for Water Electrolysis. PhD thesis, NTNU, Trondheim, Norway, 2005.
[8] K.E. Ayers, C. Capuano, B. Carter, L. Dalton, G. Hanlon, J. Manco, M. Niedzwiecki, in: Abstract 603, Polymer Electrolyte Fuel Cells 10 Symposium, 218th ECS Meeting – Las Vegas, NV, October 10-October 15, 2010.
[9] A. Marshall, S. Sunde, M. Tsypkin, R. Tunold, Int. J. Hydrogen Energy 32 (2007) 2320.
[10] C. Lamy, Operation of fuel cells with biomass resources (hydrogen and alcohols), in: Piet Lens, Christian Kennes, Pierre Le Cloirec, Marc Deshusses (Eds.), Waste Gas Treatment for Resource Recovery, IWA Publishing, London, 2006, pp. 360–384 (Chapter 21).
[11] V. Bambagioni, M. Bevilacqua, C. Bianchini, J. Filippi, A. Lavacchi, A. Marchionni, F. Vizza, P.K. Shen, ChemSusChem 3 (2010) 851.
[12] T. Take, K. Tsurutani, M. Umeda, J. Power Sources 164 (2007) 9.

[13] Z. Hu, M. Wu, Z. Wei, S. Song, P.K. Shen, J. Power Sources 166 (2007) 458.
[14] S.R. Narayanan, W. Chun, B. Jeffries-Nakamura, T. I. Valdez, US Patent 6533919, March 18, 2003.
[15] J. Thibault, MSc, University of Poitiers, May 2011.
[16] T. Jaubert, MSc, University of Poitiers, June 2012.
[17] A. Caravaca, F.M. Sapountzi, A. de Lucas-Consuegra, C. Molina-Mora, F. Dorado, J.L. Valverde, Int. J. Hydrogen Energy 37 (2012) 9504.
[18] P.A. Selembo, J.M. Perez, W.A. Lloyd, B.E. Logan, Int. J. Hydrogen Energy 34 (2009) 5373.
[19] A.T. Marshall, R.G. Haverkamp, Int. J. Hydrogen Energy 33 (2008) 4649.
[20] W.L. Guo, L. Li, S. Tian, S.L. Liu, Y.P. Wu, Int. J. Hydrogen Energy 36 (2011) 9415.
[21] C. Lamy, A. Devadas, M. Simoes, C. Coutanceau, Electrochim. Acta 60 (2012) 112.
[22] S. Rousseau, C. Coutanceau, C. Lamy, J.-M. Léger, J. Power Sources 158 (2006) 18.
[23] A.D. McNaught, A. Wilkinson, Compendium of Chemical Terminology, the Gold Book, second ed., Blackwell Science, New York, 1997.
[24] L. Dubau, F. Hahn, C. Coutanceau, J.-M. Léger, C. Lamy, J. Electroanal. Chem. 554/555 (2003) 407.
[25] L. Dubau, C. Coutanceau, J.-M. Léger, C. Lamy, J. Appl. Electrochem 33 (2003) 419.
[26] W.S. Rasband, Image J, U.S. National Institutes of Health, Bethesda, Maryland, USA, 1997, 2012. http://imagej.nih.gov/ij/.
[27] F. Gloaguen, N. Andolfatto, R. Durand, P. Ozil, J. Appl. Electrochem. 24 (1994) 863.
[28] C. Lamy, S. Rousseau, E.M. Belgsir, C. Coutanceau, J.-M. Léger, Electrochim. Acta 49 (2004) 3901.
[29] J.-M. Perez, B. Beden, F. Hahn, A. Aldaz, C. Lamy, J. Electroanal. Chem. 262 (1989) 251.
[30] H. Hitmi, E.M. Belgsir, J.-M. Léger, C. Lamy, R.O. Lezna, Electrochim. Acta 39 (1994) 407.
[31] F. Vigier, C. Coutanceau, A. Perrard, E.M. Belgsir, C. Lamy, J. Appl. Electrochem. 34 (2004) 439.
[32] J. Hong Kim, S.M. Choi, S.H. Nam, M.H. Seo, S.H. Choi, W.B. Kim, Appl. Catal. B: Environ. 82 (2008) 89.
[33] M. Li, W.-P. Zhou, N.S. Marinkovic, K. Sasaki, R.R. Adzic, Electrochim. Acta 104 (2013) 454.
[34] N.R. de Tacconi, R.O. Lezna, B. Beden, F. Hahn, C. Lamy, J. Electroanal. Chem. 379 (1994) 329.
[35] E. Mendez, J.L. Rodrıguez, M.C. Arevalo, E. Pastor, Langmuir 18 (2002) 763.
[36] A. Bonesi, G. Garaventa, W.E. Triaca, A.M. Castro Luna, Int. J. Hydrogen Energy 33 (2008) 3499.
[37] F. Colmati, E. Antolini, E.R. Gonzalez, J. Alloys Comp. 456 (2008) 264.
[38] H.J. Kim, S.M. Choi, S. Green, G.A. Tompsett, S.H. Lee, G.W. Huberb, W.B. Kim, Appl. Catal. B: Environ. 11 (2011) 366.
[39] M. Watanabe, S. Motoo, J. Electroanal. Chem. 60 (1975) 275.
[40] C. Lamy, E.M. Belgsir, Other direct alcohol fuel cells, in: W. Vielstich, A. Lamm, H. Gasteiger (Eds.), Handbook of Fuel Cells: Fundamentals and Survey of Systems, vol. 1, Wiley, Chichester, 2003, pp. 323–334 (Chapter 19).
[41] J. Wojtowicz, in: J.O.'M. Bokris, B.E. Conway (Eds.), Modern Aspects of Electrochemistry, vol. 8, Plenum Press, New York, 1973, p. 47.
[42] M. Hackar, B. Beden, C. Lamy, J. Electroanal. Chem. 287 (1990) 81–98.
[43] J.L. Hudson, T.T. Tsotsis, Chem. Eng. Sci. 49 (1994) 1493.
[44] M.T.M. Koper, in: I. Prigogine, S.A. Rice (Eds.), Advances in Chemical Physics, vol. 92, John Wiley & Sons, New York, 1996, p. 161.
[45] M. Krausa, W. Vielstich, J. Electroanal. Chem. 339 (1995) 7.
[46] J. Jiang, A. Kucernak, J. Electroanal. Chem. 543 (2003) 187.
[47] L. Han, H. Ju, Y. Xuand, Int. J. Hydrogen Energy 37 (2012) 15156.
[48] M.T.M. Koper, M. Hachkar, B. Beden, J. Chem. Soc. Faraday Trans. 92 (1996) 3975.